Atmospheric Environment 338 (2024) 120849

Contents lists available at ScienceDirect

Atmospheric Environment

journal homepage: www.elsevier.com/locate/atmosenv

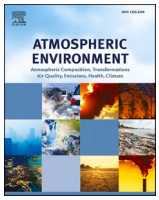

Gaseous and aerosol emissions from open burning of tree pruning and hedge trimming residues: Detailed composition and toxicity

A. López-Caravaca [a], E.D. Vicente [b], D. Figueiredo [b], M. Evtyugina [b], J.F. Nicolás [a], E. Yubero [a], N. Galindo [a], Jiří Ryšavý [c], C.A. Alves [b,*]

[a] Atmospheric Pollution Laboratory (LCA), Department of Applied Physics, Miguel Hernández University, Avenida de la Universidad S/N, 03202, Elche, Spain
[b] Centre for Environmental and Marine Studies, Department of Environment, University of Aveiro, 3810-193 Aveiro, Portugal
[c] VSB – Technical University of Ostrava, Centre for Energy and Environmental Technologies, Energy Research Centre, 17. Listopadu 2172/15, 708 00, Ostrava, Poruba, Czech Republic

HIGHLIGHTS

- EFs of gaseous pollutants and PM_{10} for the open burning of pruning wastes were obtained.
- PM_{10} was dominated by organic carbon, 50% of which was found to be water soluble.
- All samples significantly reduced the viability of alveolar epithelial cells.
- PAHs and saccharides were significantly correlated with cell viability.
- WSOC and some PAHs correlated with OP^{DTT}, while OP^{AA} was linked to some trace metals.

ARTICLE INFO

Keywords:
PM_{10}
Open burning
Gaseous emissions
Oxidative potential
Cell viability

ABSTRACT

Gaseous and PM_{10} samples were collected during the open burning of pruning residues (olive branches and garden waste) and characterised by distinct analytical techniques to obtain comprehensive chemical emission profiles. Oxidative potential (dithiothreoitol and ascorbic acid assays) and cell viability tests were also performed with the aim of evaluating aerosol toxicity. Emission factors (EFs) were as follows (g kg^{-1} biofuel, dry basis): 1537–1672 for CO_2, 41.9–80 for CO, 2.74–6.6 for CH_4, 0.89–3.51 for ethane, 0.79–1.78 for ethylene and 0.56–3.47 for formaldehyde. Emissions of PM_{10}, organic carbon (OC) and elemental carbon (EC) were in the ranges 8–41, 3–18, and 0.4–1.5 g kg^{-1} biofuel, dry basis, respectively. OC accounted for 35–45% of the total PM_{10} mass, while EC contributed between around 3% and 5%. WSOC/OC ratios varied from 0.4 to 0.6, revealing that a substantial portion of the carbon emitted was hydrosoluble. Water soluble ions constituted around 8–21% of the PM_{10} mass, with potassium and chloride as the most abundant ions in all samples. Levoglucosan, widely used a reliable biomass burning tracer, was found in significant amounts in all samples (up to 1.2% of the PM_{10} mass). Retene, generally pointed out as a biomass combustion biomarker, was the predominant PAH. WSOC and some PAHs showed significant positive correlations with the intrinsic OP measured with the DTT assay, while the OP^{AA} was significantly correlated with some trace metals, such as Fe or Ni. All samples significantly reduced the viability of alveolar epithelial cells.

1. Introduction

The harmful impacts of particulate matter (PM) on human health, ecosystems, cultural heritage and climate are well known (Andreae, 2019; Comite et al., 2021; Lelieveld et al., 2019; Ren-Jian et al., 2012; van der Werf et al., 2017). These effects depend on the physico-chemical properties of PM (mainly size and chemical composition), which in turn are a function of its sources and formation processes.

Biomass burning has attracted increasing attention in recent years as a source of PM due to the widespread use of wood for residential heating in many rural, suburban and urban areas worldwide (Chen et al., 2017; Vicente and Alves, 2018; Weber et al., 2019). Furthermore, unlike

* Corresponding author.
E-mail address: celia.alves@ua.pt (C.A. Alves).

https://doi.org/10.1016/j.atmosenv.2024.120849
Received 11 July 2024; Received in revised form 11 September 2024; Accepted 28 September 2024
Available online 1 October 2024

emissions from many other sources of air pollution, biomass combustion emissions are increasing worldwide (Chen et al., 2017; Vicente and Alves, 2018). Exposure to biomass smoke has been linked with cardiovascular and respiratory diseases (Karanasiou et al., 2021; Sigsgaard et al., 2015), as well as with increased mutagenic activity (Johnston et al., 2019; Van Den Heuvel et al., 2018), thus causing similar health outcomes to traffic PM. The adverse health effects associated with biomass burning emissions are due to hazardous substances such as polycyclic aromatic hydrocarbons (PAHs) and their derivatives, which are carcinogenic (Ravindra et al., 2008). The production of reactive oxidative species (ROS) caused by particulate matter from biomass combustion in the residential sector has been found to be greater than that from other typical sources, such as diesel vehicles and power plant units (Jin et al., 2016; Wu et al., 2022a). Smoke particles also affect the earth's radiative balance and can have a significant impact on global climate change (Keywood et al., 2013; Reddington et al., 2019).

In conformity with the PKU-fuel dataset, 7900 Tg of biomass were consumed worldwide in 2019. Global primary emissions of $PM_{2.5}$, black carbon and organic carbon from biofuel combustion were around 51, 4.6 and 29 Tg, respectively, accounting for about 70%, 55% and 90% of the total emissions from all sources. The most contributing sectors were residential and agricultural waste burning (Jiang et al., 2024).

The combustion of wood and other biomass fuels, as well as crop residue burnings, also emit a variety of gaseous pollutants, including CO, CH_4 and volatile organic compounds, which can react with OH radicals and form ozone and other photochemical oxidants, thus affecting the oxidation capacity of the troposphere (Koppmann et al., 2005; Yao et al., 2023). Over the past few years, emission factors (EFs) for crop residue and domestic biomass burning have been documented (Akagi et al., 2011; Chantara et al., 2019; Desservettaz et al., 2023). These EFs have been applied to develop emission inventories for this source (Alves et al., 2019; Zhang et al., 2013).

PM and gaseous pollutant emissions from biomass burning are dependent on weather, type of biofuel, burning practices, etc. (Viana et al., 2016). Despite being banned in most regions of developed countries, biomass burning is still a regular practise for land clearing in several regions. This fact highlights the need to know the specific emission factors and chemical profiles to improve the quality of both emission inventories and source assignment models.

Numerous studies have been performed to obtain EFs of multiple pollutants from agricultural residue burning (Deshpande et al., 2023; Gonçalves et al., 2011; Ravindra et al., 2019; Sahai et al., 2007; Tian et al., 2017). However, the chemical characterisation of emissions from the burning of green garden waste is less well documented, even though this action releases large amounts of many noxious components (Alves et al., 2019). Furthermore, in ambient air, it is very difficult to distinguish between PM emissions from residential wood and green waste burning. Therefore, a better characterisation of the chemical composition of PM from the burning of green wastes is important for source apportionment studies.

Taking the above into account, libraries collecting information on PM chemical source profiles are of great value to the scientific community. The SPECIATE repository, provided by the US EPA since 1988, currently contains more than 3000 local source profiles. Short while ago, an analogous effort has been made in Europe, resulting in the SPECIEUROPE dataset portrayed by Pernigotti et al. (2016).

The aim of this study was to perform a complete chemical characterisation of PM emissions from the burning of green garden waste (pruning waste), as well as emission factors for PM and gaseous pollutants. In addition, toxicity tests of PM extracts were performed by acellular oxidative potential assays (ascorbic acid and dithiothreitol) and cellular cytotoxicity tests.

2. Methodology

2.1. Sample collection and PM_{10} measurements

The burned residues included olive (*Olea europaea*) branches from a local farmer and ornamental shrubs that are common in private and public gardens, as well as in commercial landscapes. The latter were supplied by the University of Aveiro gardening team, comprising willow (*Salix atrocinerea*), red firethorn, also known as scarlet firethorn (*Pyracanta coccinea*), wild privet (*Ligustrum vulgare*), and Chinese privet, a highly invasive East Asian species (*Ligustrum lucidum*). The experiment tried to replicate the usual procedures of land and garden owners who burn the waste in the backyard or in open fields with some grass.

A total of 6 particulate matter samples with aerodynamic diameter lower than 10 μm (PM_{10}) were gotten (Table 1). In parallel, another 6 samples of the gaseous phase were collected into Tedlar bags. The sampling time ranged between 8 and 20 min, depending on the smoke loads. A high-volume sampler (MCV, model CAV-A/mb, Spain) at a flow rate of 30 $m^3\ h^{-1}$ was employed to gather PM_{10} samples onto 150 mm diameter quartz fibre filters (Pallflex). This equipment was placed at 3–4 m from the fire and 1.3 m from the ground to be able to sample at the centre of the smoke plume. Thus, these samples represent primary aerosols that have not undergone atmospheric post-processing. The sampling method of the present study has been used previously to characterise emissions from prescribed fires (Alves et al., 2010), wildfires (e.g., Alves et al., 2011; Vicente et al., 2011, 2013) and open burning of tree pruning residues (Alves et al., 2019).

Gravimetric quantification of PM_{10} was performed using a microbalance from Radwag (model MYA 5.4Y.F1, readability of 1 μg). Before weighing, each filter was kept for 72 h at constant temperature (20 ± 1 °C) and relative humidity (50 ± 5 %) conditions, both before and after sampling. Following the propagation method described by Lacey and Faulker (2015), the overall uncertainty associated with the measurement of PM_{10} was estimated to be 4.9%.

2.2. Emission factors and chemical speciation

Following the combustion experiments, a Fourier Transform Infrared analyser (FTIR Gasmet, CX4000, Finland) was used to determine the levels of gaseous pollutants from the Tedlar bags, as detailed in Alves et al. (2019). Calibrated gases in the FTIR include CO_2, CO, N_2O, NO, NH_3, HCl, CH_4, ethylene, ethane, hexane, formaldehyde, and total organic carbon (TOC), which were quantified in the samples, and also NO_2, SO_2 and propane, which were not detected. The relative total expanded uncertainty for each of the gaseous compounds is presented in the supplementary material (Table S1). Emission factors were calculated from the values obtained in the FTIR using a carbon material balance. The emission factor (EF) for a species X is the mass of X released per mass of burnt biofuel (g kg^{-1} dry basis) and is calculated as follows:

$$EF = \frac{[X]}{\Delta[CO_2] + \Delta[CO] + \Delta[HC] + \Delta[PC]} \times 50\% \quad (1)$$

where $[X]$ is the level (g m^{-3}) of species X, $\Delta[CO_2]$, $\Delta[CO]$, $\Delta[HC]$ and $\Delta[PC]$ are concentrations in carbon equivalents (with background air

Table 1
Characteristics of the burned material and combustion stage for each sample.

Sample	Characteristics
AL-1	Background air
AL-2	Olive tree pruning branches
AL-3	Olive tree pruning branches
AL-4	Hedge trimming waste mixture
AL-5	Hedge trimming waste mixture
AL-6	Hedge trimming waste mixture

values subtracted), in g C m^{-3}, of carbon dioxide, carbon monoxide, hydrocarbons and particulate carbon ($PC = OC + EC$), respectively. A percentage of 50% is used to account for the mass fraction of carbon (g kg^{-1}) in the biofuel. Although 50% is a universally accepted mean value for plant carbon content, small percentage differences can be observed between species and between distinct parts of a tree or shrub (e.g., branches versus leaves) (Ma et al., 2018; Thomas and Martin, 2012). These variations can slightly affect the estimated emission factors.

The modified combustion efficiency (MCE) is calculated to infer the proportion between the different stages of fire combustion, especially flaming versus smouldering:

$$MCE = \frac{\Delta[CO_2]}{\Delta[CO_2] + \Delta[CO]} \quad (2)$$

The concentrations of organic carbon (OC) and elemental carbon (EC) were quantified in a thermo-optical transmission (TOT) equipment using two 11 mm circles taken from the PM_{10} filters and following the EUSAAR-2 protocol (Pio et al., 2011).

The elemental composition of PM_{10} samples was determined on 47-mm diameter filter punches employing an energy dispersive X-ray fluorescence (ED-XRF) technique, which is described in detail in Chiari et al. (2018). It is a non-destructive technique, so the portion of filter used for this analysis was subsequently used for further determinations.

To determine the concentration of water-soluble organic carbon compounds (WSOC), a 4.3 cm^2 circle of each filter was ultrasonically extracted with 15 ml of ultrapure water for 45 min. The extracts were filtered through 0.45 μm pore size syringe filters to eliminate fibres derived from the filters and other insoluble materials. An organic carbon analyser TOC-L CSH (Shimadzu) with a highly sensitive catalyst was used. The WSOC and TC (total soluble carbon) content was determined by the NPOC (non-purgeable organic carbon) method. This method uses 1 M HCl (PanReac AppliChem) to acidify the sample and pure air (Air-Liquid) to remove dissolved inorganic carbon and volatile organic compounds. The standard used to determine the concentration of organic carbon was potassium hydrogen phthalate (PanReac AppliChem). Each sample was measured twice, and the mean of the resulting concentrations was calculated. An injection volume of 500 μl was used. The repeatability between samples was 97–99% and all samples showed concentrations above the minimum detection limit (MDL).

Two 19 mm diameter filter punches were extracted with 4 ml of Milli-Q ultrapure water by ultrasonication for 30 min. The extracts were subsequently filtered (0.2 μm pore size PVDF syringe filter, Whatman™) and analysed by ion chromatography. Of these extracts, two parts were used for the determination of water-soluble ions and a third part was devoted to the determination of the sugar content. Water-soluble ions were measured with a DIONEX ICS-5000+ ion chromatograph. A DIONEX Ionpac AS11-HC-4 μm (2 × 250 mm) analytical column and potassium hydroxide (30 mM) as eluent were used for the determination of anions. The analytical column used for cation analysis was a DIONEX Ionpac CS16 (3 × 250 mm). The eluent was 30 mM methanesulfonic acid. The calibration curves were obtained with 8 different concentrations for the various ions.

Carbohydrates were analysed by high-performance anion exchange chromatography with pulsed amperometric detection (HPAE-PAD) in an instrument from Thermo Fisher Scientific (Waltham, MA, USA), model DionexTM ICS-5000+, equipped with a Dionex ED50 detector, which integrates a disposable gold electrode and a reference pH electrode. Both system control and data processing were carried out through the Chromeleon software. The chromatographic system was equipped with a Carbopac PA-1 analytical column to separate the various carbohydrates. Three eluents were employed for the mobile phase: eluent A-ultrapure water, eluent B-200 mM NaOH and eluent C-5 mM NaOH. Further details on the analytical procedure are given in Gonçalves et al. (2021).

Two 47 mm diameter circles taken from each PM_{10} filter were solvent-extracted and separated into distinct organic families in a silica gel adsorbent flash chromatography column. The extraction, fractionation and analysis for the determination of particulate organic compounds was performed following the protocol reported by Alves et al. (2011). The fractionated extracts were analysed by gas chromatography–mass spectrometry (GC model 7890B, MS model 5977A, GC Sampler 80, Agilent Technology Inc.) with a TRB-5MS 60 m × 0.25 mm × 0.25 μm column.

2.3. Oxidative potential assays

An 8.7 cm^2 punch of each PM_{10} sample was ultrasonically extracted for 45 min with 14 ml of ultrapure water. Extracts were filtered through a 0.45 μm pore size syringe filter and analysed using two acellular assays: the dithiothreitol (DTT) and ascorbic acid (AA) methods. A detailed description of OP measurements using both methods is reported in Clemente et al. (2023). Samples and blank filters were analysed in duplicate. The differences between duplicates were always less than 10%. Normalised OP^{AA} and OP^{DTT} values per cubic meter (nmol min^{-1} m^{-3}) were determined from the AA and DTT depletion rates, respectively. Mass-normalised OP activities (nmol min^{-1} μg^{-1}) were also calculated.

2.4. Sample preparation for toxicological analysis

To determine cell viability of PM_{10} from the combustion of olive branches and hedge trimming waste mixtures, samples were extracted for 24 h with methylene chloride followed by two extractions with methanol for 10 min each in an ultrasonic bath. The total organic extracts were then filtered and reduced to a volume lower than 1 ml in a Turbo Vap® II concentration station (Biotage). This volume was transferred to a glass vial, dried with a stream of nitrogen and then suspended into dimethyl sulfoxide (DMSO).

2.5. Cell culture and cytotoxicity assays

For the cytotoxicity assay, the A549 cell line (human lung adenocarcinoma epithelial cells) were cultured at 37 °C in a humidified atmosphere with 5% CO_2. Cells were maintained in Kaighn's Modification of Ham's F-12 Medium (F-12 K – PAN-Biotech GmbH, Germany) supplemented with 10% (v/v) fetal bovine serum (FBS), 1% of penicillin–streptomycin and 1% amphotericin-B (all from PAN-Biotech GmbH, Germany). Cell viability was assessed using the colorimetric MTT (3-(4,5-dimethyl-2-thiazolyl)-2,5-diphenyl-2H-tetrazolium bromide) assay (Thermo Fisher Scientific). A549 cells were seeded in 96-well plates at a density of 4×10^4 cells ml^{-1} (4×10^3 cells per well) and allowed to adhere for 24 h. The medium was then substituted by six concentrations of PM_{10} extract (6.25, 12.5, 25, 50, 100 and 200 μg ml^{-1}) in triplicate. In addition to the control group (cells and culture medium), a solvent control treated with the same percentage of DMSO at the maximum tested concentration was also included. Neither control group showed any effect on the reduction of viability. After the exposure period of 24 h, 50 μl of MTT (1.0 mg ml^{-1} in phosphate-buffered saline) was added to each well and incubated at culture conditions for 4 h to allow the production of formazan crystals. Following this time, the MTT-containing medium was eliminated and 150 μl of DMSO was added. The samples were kept for 2 h at room temperature in the dark, shaking gently to facilitate the dissolution of the crystals. The absorbance at 570 nm was then recorded in a microplate reader (Synergy HT® Multi-Mode; BioTek®, Winooski, VT, USA).

2.6. Statistical analysis

Statistical analysis of the data was carried out using the SPSS software (IBM SPSS statistics version 29). The Shapiro-Wilk normality test and the Levene's test for homogeneity of variances were applied. Data from the MTT assay for particulate samples were compared with the corresponding controls using firstly the Kruskall-Wallis non-parametric

test and then the Dunn's post hoc test and Bonferroni's p-value adjustment. The concentrations that caused 50% (EC50) of cytotoxicity in A549 cells were obtained by fitting a triparametric sigmoidal logistic function to the dose-response curve. Spearman correlations with a significance level of 95% or 99% were also conducted with the SPSS software to evaluate the relationship between toxicological outcomes (EC50 and OP) and PM_{10}-bound constituents.

3. Results

3.1. Modified combustion efficiency and emission factors

MCE values ranged from 0.924 for olive branches to 0.962 for hedge trimming residues (Table 2). An MCE close to 1 suggests pure flaming, while values near 0.8 reflect intense smouldering conditions. A value near 0.9 indicates roughly equal proportions of biofuel consumption by flaming and smouldering (Akagi et al., 2011). Olive samples emitted a lower percentage of CO_2 and a higher proportion of CO than those from the combustion of hedge trimming waste mixtures. In PM_{10} samples from the burning of olive branches, on average, 88% of the carbon emitted was in the form of CO_2, while for hedge trimming samples the proportion ranged between 92 and 95%. The thinner branches of the bushes burn better. Thus, greater combustion efficiency leads to higher CO_2 emissions. On the other hand, CO for the olive samples accounted for 6–7% of the carbon emitted, while lower values, between 3.7 and 5.5%, were obtained for the combustion of hedge trimming waste mixtures. A higher CO EF and a lower MCE value for the second olive branch burning sample are indicative of increased contribution of smouldering emissions. The percentage of particulate carbon emitted was much higher for olive samples, approximately 4%, compared to that of the smoke from burning mixtures of various shrubs, for which PC represented between 0.6 and 2.3% of the total carbon emitted. These results suggest that the differences in emissions may be due to the different physicochemical properties of the fuels, such as size and specifically moisture. Likewise, the EFs for PM, EC and OC (40, 1.4 and 18 g kg^{-1}, respectively) from the burning of olive branches obtained in this study are higher with respect to previous work developed in the same area of study (Alves et al., 2019; 17, 1.2 and 7.4 g kg^{-1}, respectively). Other factors contributing to differences in emissions may be oxygen supply, fuel arrangement (piled up or spread out), weather conditions, among others (Hayashi et al., 2014; Oanh et al., 2011).

CO_2 EFs for olive samples were 1562 and 1537 g kg^{-1}, while samples that included wastes from hedge trimming resulted in higher values, from 1612 to 1672 g CO_2 kg^{-1}, increasing as combustion developed. However, the highest EFs of CO (67 and 80 g CO kg^{-1}) were registered for the combustion of olive branches, whereas values for burning branches of various types of shrubs were almost 50% lower (62, 59 and 42 g CO kg^{-1}). As expected, CO_2 emissions increased linearly with combustion efficiency, so an excellent correlation between the MCE values and the EFs of this greenhouse gas was obtained (r = 0.97). The opposite was observed for CO, which was negatively correlated with MCE (r = −1.0). Flaming combustion involves the fast reaction of O_2 with gaseous compounds emitted from the solid biofuel and is frequent in small-diameter dry aerial biomass or foliage. During flaming combustion, the carbon in the fuel is converted into highly oxidised gaseous species such as CO_2, and most EC particles are generated. As combustion approaches completion, the smouldering phase becomes predominant. Slow combustion generates CO, CH_4, non-methane hydrocarbons and primary organic aerosols (Akagi et al., 2011). The dependence on combustion efficiency is clearly demonstrated by the relationships between MCE and EFs of PM_{10} (r = −0.91), OC (r = −0.87), TOC (r = −0.97) and ethane (r = −0.96). PM_{10} EFs were positively correlated with those of the different forms of organic carbon in the gas (TOC) and particulate (OC) phases, with Pearson correlation coefficients of 0.89 and 1.0, respectively, suggesting that these atmospheric constituents are co-emitted in identical proportions.

Methane EFs found in this study varied between 2.7 and 6.6 g kg^{-1}, with the highest value being recorded for the burning of olive branches. The values obtained by Alves et al. (2019), for the open burning of wastes from tree pruning, were within the same range (2.06–5.8 g CH_4 kg^{-1}). The highest values were also observed for olive tree samples. Ethane (C_2H_6) and formaldehyde (CHOH) EFs were higher for the combustion of olive residues than for the hedge trimming waste mixtures. In the case of ethylene (C_2H_4) and hexane (C_6H_{14}), no clear distinction was observed between EFs for the various types of residues, although slightly higher values were observed for the PM_{10} sample with the lowest MCE value. Ammonia (NH_3) was not detected in any of the samples.

The EFs of this work (Table 3) are within the ranges reported for forest fires or residual biomass burning with higher proportion of flaming conditions than smouldering. However, comparisons between studies should be made with some caution given the differences in experimental strategies, mainly open burn vs. combustion tests in laboratory chambers. Agaki et al. (2011) argued that "fresh" emissions sampled in the field can produce similar EFs for trace gases compared to lab experiments at the same MCE. Nevertheless, such controlled experiments do not usually reproduce realistic combustion conditions in the field. In general, in laboratory testing the biofuels are more aged and drier and therefore their moisture content is lower than that of biomass in the field. On the other hand, wind conditions in the field cannot be reproduced in the laboratory (Andreae, 2019).

Table 2
Emission factors for each sample (g kg^{-1}, dry basis).

	AL-2	AL-3	AL-4	AL-5	AL-6
MCE	0.937	0.924	0.943	0.946	0.962
CO_2	1562	1537	1612	1627	1672
CO	67.2	80	62.3	59.3	41.9
N_2O	ND	0.21	0.17	0.28	0.66
NO_x as NO_2	15	27.4	16.1	9.6	8.82
HCl	0.51	0.36	0.02	0.04	0.75
HF	0.02	ND	0.01	0.02	0.03
CH_4	2.74	6.60	4.15	3.13	2.91
C_2H_6	2.93	3.51	1.84	0.89	ND
C_2H_4	1.07	1.78	0.79	1.01	1.19
C_3H_8	ND	ND	0.01	0.05	0.06
C_6H_{14}	0.23	0.8	0.54	0.23	0.37
CHOH	3.47	2.24	0.97	1.21	0.56
TOC	7.72	11.2	6.5	4.84	3.41
OC	18.5	17.1	8.14	6.6	2.9
EC	1.45	1.3	0.91	0.53	0.4
PM_{10}	40.9	40.1	21.6	19.1	8.33

SO_2, NH_3, C_3H_6, CH_3OH: not detected.

3.2. Chemical composition of PM_{10}

Concentrations of elements and major carbonaceous components in biomass burning samples are given in Table 4. The data shown in this table are expressed in mass fractions.

OC represented between 35 and 45%, while EC accounted for 3–5% of the total PM_{10} mass. The highest OC mass fractions were found in samples from olive burning, while those of EC occurred in the hedge trimming mixture samples. The OC/EC ratios obtained in the present work varied from 7.3 to 13.2, averaging 10.8. The highest ratios corresponded to the burning of olive branches, while the lowest values were found for hedge trimming residues. These results are consistent with those from previous research showing that OC/EC ratios for vehicle emissions (from 0.02 to 2.36) are lower than those for coal and biomass combustion (between 1.1 and 60.5; Pio et al., 2011; Pani et al., 2019).

The WSOC/OC ratio can be employed to assess the origin of organic carbon (Boreddy et al., 2018; Kondo et al., 2007). Emissions from biomass burning are characterised by a high WSOC/OC ratio (Mayol-Bracero et al., 2002) since a substantial fraction of the OC emitted during biomass combustion is water-soluble (Graham et al.,

Table 3
Comparison of the emission factors (g kg^{-1}, dry basis) of the present study with those reported in bibliography for agricultural burning and forest fires.

MCE	Measu-rements	CO_2	CO	CH_4	PM	OC	EC	Type of biomass burning	Reference
0.94 ± 0.01	Field	1602 ± 53.5	62.1 ± 13.8	3.9 ± 1.6	26.0 ± 14.1[a]	10.6 ± 6.8	0.92 ± 0.46	Tree pruning and hedge trimming residues	This study
>0.95	Field	1564–1663	40.6–78.7		8.8–16.9[a]	2.7–7.4	0.32–1.18	Olive, willow, vine and acacia branches	Alves et al. (2019)
0.94 ± 0.02	Field	1660 ± 90	69 ± 20	2.7 ± 2.2	6.7 ± 3.3[b]	3.0 ± 1.5	0.53 ± 0.35	Savanna and grassland	Andreae (2019)
0.92 ± 0.06	Field	1430 ± 230	76 ± 55	5.7 ± 6.0	8.2 ± 4.4[b]	4.9 ± 3.6	0.42 ± 0.28	Agricultural residues	Andreae (2019)
0.91 ± 0.03	Field	1620 ± 70	104 ± 39	6.5 ± 1.6	8.3 ± 3.3[b]	4.4 ± 1.9	0.51 ± 0.34	Tropical forest	Andreae (2019)
0.90 ± 0.05	Field	1570 ± 130	113 ± 50	5.2 ± 2.8	18.5 ± 14.4[b]	10.9 ± 7.2	0.55 ± 0.36	Temperate forest	Andreae (2019)
0.89 ± 0.04	Field	1530 ± 140	121 ± 47	5.5 ± 2.5	18.7 ± 15.9[b]	5.9 ± 2.5	0.10 ± 0.09	Boreal forest	Andreae (2019)
0.91 ± 0.03	Lab	1311 ± 181	47.9 ± 13.5		11.4 ± 4.9[b]	5.1 ± 3.0	0.24 ± 0.12	Wheat straw	Ni et al., 2017
0.93 ± 0.03	Lab	1393 ± 91	57.2 ± 26.0		8.5 ± 6.7[b]	3.3 ± 2.8	0.21 ± 0.13	Rice straw	Ni et al., 2017
0.93 ± 0.02	Lab	1363 ± 154	52.1 ± 17.7		12.0 ± 5.4[b]	6.3 ± 3.6	0.28 ± 0.09	Corn stalk	Ni et al., 2017
0.91 ± 0.03	Lab				13.1[b]	5.6	1.38	Wheat straw	Zhang et al. (2017)
0.93 ± 0.03	Lab				6.2[b]	5.3	0.55	Rice straw	Zhang et al. (2017)
0.93 ± 0.02	Lab				10.5[b]	6.3	0.94	Corn straw	Zhang et al. (2017)
0.930 ± 0.020	Aircraft	1403 ± 22	71 ± 13	3.17 ± 0.95	21.47 ± 6.95[c]	9.88 ± 3.35	0.120 ± 0.052	Crop residues	Travis et al. (2023)
0.902 ± 0.032	Aircraft	1666 ± 44	113 ± 25	7.48 ± 2.03	20.97 ± 6.09[c]	10.14 ± 2.97	0.219 ± 0.132	Prescribed fires of slash and piles	Travis et al. (2023)
0.897 ± 0.012	Aircraft	1506 ± 23	113 ± 13	4.52 ± 0.74	29.19 ± 4.29[c]	14.22 ± 2.02	0.309 ± 0.154	Grassland	Travis et al. (2023)
0.87–0.97	Lab	1052–1851	33.3–156	1.95–5.46	1.77–21.6[a]	0.54–11.1	0.19–0.47	Crop residues	Santiago de la Rosa et al. (2018)
0.96 ± 0.01	Lab	1618 ± 108	25.7 ± 2.04	2.29 ± 0.13	1.81 ± 0.14[a]	0.67 ± 0.36	0.37 ± 0.10	Sugarcane	Mugica-Álvarez et al. (2018)

[a] PM_{10}.
[b] $PM_{2.5}$.
[c] PM_1 calculated by mass balance from chemical species measured by HR-ToF-AMS in an aircraft.

Table 4
Elemental composition and main carbonaceous components in PM_{10} samples (wt.%) from the combustion of tree pruning and hedge trimming wastes. bdl: below detection limit.

	AL-2	AL-3	AL-4	AL-5	AL-6
Ti	0.004	0.012	0.009	0.004	0.02
Cr	bdl	bdl	bdl	bdl	bdl
Mn	0.03	0.11	0.11	bdl	bdl
Fe	0.02	0.07	0.07	0.06	0.15
Ni	0.05	0.2	0.14	0.1	0.4
Cu	bdl	bdl	bdl	bdl	0.02
Zn	0.2	0.3	0.6	0.6	1.4
As	bdl	bdl	bdl	bdl	bdl
Br	0.025	0.015	0.016	0.056	0.043
OC	45.33	42.61	37.61	34.62	34.8
EC	3.55	3.24	4.22	2.80	4.76
TC	48.88	45.85	41.82	37.42	39.56
WSOC	18.72	18.11	16.60	14.64	21.38

2022). When no emissions from biomass burning are recorded, a higher WSOC/OC ratio is indicative of organic aerosols transported over long distances. WSOC/OC ratios between 0.06 and 0.27 are typical of vehicle emissions (Cheung et al., 2009; Saarikoski et al., 2008), while higher values (>0.5) are associated with biomass burning aerosols (Rajput et al., 2013; Ramya et al., 2023). In the present study, the WSOC/OC ratio varied between 0.4 and 0.6.

Mass percentages for the analysed ions are shown in Table S2 included in the supplementary material. Water soluble ions represented about 8–21% of the total PM_{10} mass emitted during biomass burning. Potassium and chloride were the most abundant ions in all samples, accounting for 2.7–7.7% and 2.8–8.8%, respectively, of the total ion concentrations, followed by sulphate. It is well known that a large amount of the inorganic fraction of biomass burning emissions consist of soluble potassium salts, such as KCl or K_2SO_4 (Jing et al., 2017; Vasilakopoulou et al., 2023). Calcium and sodium, which are essential elements in the structure of plants (Pinto et al., 2016), were also present in significant amounts in all samples. The most abundant heavy metals in biomass burning samples were Zn, Ni and Fe. Mn was also detected in significant amounts in three of the samples. Zn, which plays a key role in the enzyme structure of plants (Pinto et al., 2016), has been found to be abundant in PM samples from biomass burning in chamber experiments (Akbari et al., 2021; Wu et al., 2022b). Fe and Ni were also detected in high concentration in particles emitted during biomass combustion (Das et al., 2019; Wu et al., 2022b).

In this study, more than 120 organic compounds were quantified in the PM_{10} samples (Table 5). Sugars and polyols, followed by acids, represented the most abundant families.

Levoglucosan, followed by its stereoisomers mannosan and galactosan, represented the largest mass fraction of PM_{10} (Fig. 1). These compounds result from the thermal decomposition of cellulose (levoglucosan) and hemicellulose (mannosan and galactosan) when combustion occurs at temperatures above 300 °C (Bhattarai et al., 2019; Li et al., 2021). Poor correlations between the three isomers indicate differences in biofuel polymeric compositions and combustion efficiencies for each sample (Zhu et al., 2015). Other sugars detected in all smoke samples were glucose, mannose and xylose. Unlike anhydrosugars, emissions of the sugar alcohol myo-inositol decreased in the smouldering phase. Although levoglucosan has been pointed out as a specific biomass burning tracer, it cannot be employed alone to discern the type of biofuel burned. Instead, the ratios between levoglucosan and its isomers can help differentiate biomass source categories (hardwoods, softwoods, crop residues, etc.) (Engling et al., 2009; Sang et al., 2013; Yan et al., 2015). Cellulose and hemicellulose are the two most copious biopolymers, accounting for 40–50% and 25–35% of the weight of dry wood, respectively (Chen, 2014). Therefore, combustion of softwoods

Table 5
Speciation of PM_{10}-bound organic compounds (μg g^{-1} PM_{10}).

	AL-2	AL-3	AL-4	AL-5	AL-6
SUGARS & POLYOLS					
Myo-Inositol	720	280	540	470	bdl
Erythritol	600	bdl	330	160	120
Levoglucosan	3720	7000	8600	6600	11900
Mannosan	610	440	770	570	1020
Galactosan	770	1170	880	1000	1490
D-(+)-Glucose	140	40	600	50	60
D-(+)-Mannose + D-(+)-Xylose	20	29	16	43	3
PAHs & QUINONES					
Naphthalene	bdl	182	bdl	bdl	bdl
Acenaphthylene	bdl	bdl	bdl	bdl	bdl
2,6-Di-tert-butyl-1,4-benzoquinone	49.2	337	2.09	2.97	1260
Acenaphthene	–	–	–	–	–
Fluorene	0.854	14.4	–	12.3	61.5
9-Fluorenone	10.0	21.1	9.83	21.2	36.2
Phenanthrene	12.0	10.8	3.41	4.05	10.9
Anthracene	1.82	2.56	1.14	0.96	2.25
Carbazole	15.0	28.7	21.5	22.4	26.8
Xanthone	–	–	–	–	–
Acenaphthenequinone	–	–	–	–	–
2-Methylanthracene	49.6	3.29	1.50	1.48	2.55
9,10-Phenanthrenequinone	–	–	–	–	–
Fluoranthene	49.0	54.1	48.6	36.4	52.4
Pyrene	43.7	39.3	31.1	22.8	37.4
Retene	–	579	321	274	421
1-Methylpyrene	7.48	6.50	5.18	12.9	6.94
Benzo[a]anthracene	13.6	12.0	11.5	5.46	16.1
Chrysene	22.6	19.4	18.9	12.8	27.8
Benzo[a]anthracene-7,12-dione	–	–	3.19	–	–
5,12-Naphthacenequinone	–	–	–	–	–
Benzo[b]fluoranthene	21.3	13.8	19.3	6.92	19.4
Benzo[k]fluoranthene	0.226	8.85	2.29	1.14	4.97
7,12-Dimethylbenz[a]anthracene	–	–	–	–	–
Benzo[a]pyrene	7.87	7.17	8.02	2.65	16.4
Perylene	3.51	–	0.928	3.48	–
Indeno[1,2,3-cd]pyrene	10.5	4.54	10.0	2.54	8.84
Dibenzo[a,h]anthracene	2.93	2.81	3.07	1.16	5.59
Benzo[g,h,i]perylene	6.65	4.24	6.73	2.72	6.94
PHENOLICS & OTHER HYDROXYL COMPOUNDS					
Benzyl alcohol	281	45.6	1903	44.4	106
Benzoic acid	58.2	71.4	26.8	55.4	14.1
Catechol	1030	48.8	43.1	800	482
4-Hydroxybenzaldehyde	389	81.0	15.1	115	399
Resorcinol	194	99.6	87.7	115	215
2,4-Di-tert-butylphenol	577	25.0	–	12.2	–
4-Methyl catechol	199	2.13	2.01	78.8	75.0
4-Methylsyringol	45.3	–	–	14.2	33.8
2,6-Dimethoxyphenol	240	0.836	4.25	113	118
Orcinol	84.0	36.0	26.8	41.0	68.5
Methylresorcinol	34.2	39.5	21.6	41.0	60.2
3-Hydroxybenzoic acid methyl ester	12.4	10.9	–	8.33	28.0
4-Hydroxybenzyl alcohol	29.5	24.6	17.3	27.8	38.7
Vanillin	55.6	64.0	32.2	104	260
Pyrogallol	14.6	–	5.65	26.8	21.2
4-Ethylsyringol	36.5	–	–	11.4	–
3-Hydroxybenzoic acid	293	–	152	141	183
4-Hydroxyphenylethanol	602	235	142	194	1259
Isoeugenol	–	–	–	1.01	2.52
2-Methoxy-4-propylphenol	23.4	–	–	3.64	138
4-Propenylsyringol	231	–	–	–	–
4-hydroxybenzoic acid	65.8	139	68.0	342	722
Syringaldehyde	19.2	–	–	236	2249
Syringic acid	207	142	155	79.0	–
Vanillic acid	179	190	116	101	159
3,4-Dimethoxyphenethyl alcohol	948	–	–	–	267
Phenylbenzene	–	51.5	–	26.6	–
ALIPHATIC ALCOHOLS					
1-Pentadecanol	2.49	0.888	11.3	2.05	2.71
Octadecan-1-ol (Stearyl alcohol)	258	–	6.61	96.0	–
Hexadecanol	22.9	21.9	24.0	12.3	10.1
1-Heptacosanol	8.51	4.04	–	18.7	19.0
1-Octacosanol	118	47.8	71.4	153	249
Eicosanol	–	–	–	3.36	6.47
1-Docosanol (Behenyl alcohol)	8.92	9.26	9.96	12.9	41.1
1-Tricosanol	4.27	3.80	3.35	5.84	9.04
C24 alcohol	23.4	18.5	38.8	46.7	120
1-Pentacosanol	32.2	7.37	54.0	51.4	16.4
C26 alcohol	178	–	107	203	382
C29 alcohol	30.7	–	46.4	122	92.8
1-Tricontanol	33.9	27.9	274	606	508
C31 alcohol	–	–	29.7	63.4	83.6
STEROIDS					
Cholesterol	3.41	11.0	4.05	4.58	11.1
Stigmasterol	41.0	135	14.2	70.0	136
b-Sitosterol	295	289	53.2	187	419
Stigmast-4-en-3-one	31.2	47.1	–	34.3	44.4
Stigmasta-3,5-diene	13.8	–	6.75	–	–
CARBOXYLIC ACIDS					
Octanoic (caprilic) acid	22.5	24.6	1.29	15.4	5.19
Nonanoic (pelargonic) acid	46.6	106	15.9	17.0	38.8
Decanoic (caproic) acid	17.1	24.0	8.36	19.7	3.46
Dodecanoic (lauric) acid	61.7	57.3	2.23	49.5	55.9
Tetradecanoic (myristic) acid	62.4	135	27.6	80.0	54.5
Pentadecanoic acid	1.39	58.6	24.5	45.2	42.6
Hexadecanoic (palmitic) acid	964	1705	781	856	876
Heptadecanoic acid	35.1	38.7	22.9	31.9	28.2
Octadecanoic (stearic) acid	297	184	160	241	114
C21 acid	–	–	–	–	60.5
Docosanoic (behenic) acid	89.8	24.8	97.8	97.1	157
C23 acid	–	–	22.9	–	49.7
C24 acid	62.8	–	114	113	158
C25 acid	–	–	–	–	55.5
Hexacosanoic acid	22.77	2.58	93.4	41.8	92.4
C28 acid	–	–	105	–	123
C31 acid	–	–	112	–	246
DICARBOXYLIC ACIDS					
Butanedioic (succinic) acid	2543	5776	2008	11713	1098
1.5-Pentanedioic (glutaric) acid	–	547	283	145	243
Butanedioic (L-(−)-malic) acid	165	382	273	92.3	248
Fumaric acid (2-Butenedioic acid)	526	786	559	121	–
Hexanedioic (adipic) acid	167	385	224	170	404
Octanedioic (suberic) acid	48.2	88.7	34.2	–	–
Nonanedioic (azelaic) acid	147	288	133	53.2	85.4
Eicosanoic (arachidic) acid	42.2	32.3	47.3	38.3	52.3
Ethylmalonic acid	471	941	390	50.7	333
2-Hydroxyglutaric acid	238	324	175	97.5	170
OTHER ACIDS					
Levulinic acid	88.5	361	98.5	113	84.1
2-Furoic acid	381	274	112	165	215
Hydracrylic acid	1700	226	93.9	50.2	–
3-hydroxybutanoic ((R)-3-hydroxybutyric) acid	26.2	513	272	272	306
Glyceric acid	175	254	136	56.0	21.9
3,4-Dihydroxybutanoic acid	453	613	304	37.5	–
Citric acid	263	658	396	153	1862
9-cis-Hexadecenoic (linoleic) acid	–	–	129	85.2	83.5
cis-9-Octadecenoic (oleic) acid	122	60.0	95.0	68.1	84.5
Hexanedioic acid, bis(2-ethylhexyl) ester	–	151	65.5	68.2	191
Dehydroabietic acid	–	–	1.68	–	2.18
ACIDS METHYL ESTERS					
Tetradecanoic acid, 1-methylethyl ester (Myristic acid isopropyl ester)	–	37.8	21.9	25.6	53.8
Hexadecanoic acid, methyl ester (Palmitic acid methyl ester)	47.2	90.9	82.8	65.1	144

(*continued on next page*)

Table 5 (*continued*)

	AL-2	AL-3	AL-4	AL-5	AL-6
Isopropyl palmitate	3.38	–	5.59	1.33	–
9,12-Octadecadienoic acid methyl ester	49.5	44.7	54.8	31.3	118
9-Octadecenoic acid (Z)-, methyl ester (Oleic acid methyl ester)	87.5	107	112	66.2	204
Octadecanoic acid methyl ester (Stearic acid methyl ester)	22.9	19.0	25.7	20.8	29.1
Eicosanoic acid methyl ester	5.29	6.42	6.13	4.53	83.6
Docosanoic acid methyl ester	9.42	7.31	8.20	6.75	19.1
Tetracosanoic acid methyl ester	–	–	8.70	67.5	22.8
4-Hydroxybenzoic acid methyl ester	–	–	18.9	18.9	–
GLYCERIDIC COMPOU0S					
Glycerol	4.97	1166	587	546	98.2
1-Monopalmitin	109	–	131	–	–
1-Monostearin	292	1034	3926	–	43.0
2-Monostearin	–	–	114	–	–
OTHER COMPOU0S					
Hydroquinone	1121	478	200	464	31.3
3-Hydroxyacetophenone	44.3	29.7	32.7	32.6	56.1
4-Hydroxyacetophenone	31.4	37.6	46.3	119	–
tris(2,4-di-tertbutylphenyl) phosphate	2815	1581	2007	18219	4074
7,9-di-tert-butyl-1-oxaspiro[4,5] deca-6,9-diene-2,8-dione	101	9.69	3.36	3.58	37.0
Irganox 1076	131	297	63.3	49.0	186
1,2-Diphenylethane (Dihydrostilbene)	–	125	–	70.6	–

Xylitol, Arabitol, Ribitol + Sorbitol, D-Mannitol, Arabinose, Galactose, Fructose and Sucrose: never detected. bdl – below detection limit. The dash means the compound was not detected.

typically generates higher mannosan and galactosan emissions than hardwoods because the ratio of hemicellulose to cellulose is higher in softwoods than in hardwoods (Fine et al., 2001). Engling et al. (2006) reported values for the levoglucosan/mannosan ratio between 2.6 and 5 for softwood smoke, while a range from 13.8 to 52.3 was described as characteristic for hardwood. In addition, Schmidl et al. (2011) documented much lower ratios for softwood combustion (2.5–3.5) and higher ratios for hardwood combustion (14–17). A ratio of 26.6 was documented for the field burning of rice straw (Engling et al., 2009). In the present study, the levoglucosan/mannosan ratios ranged between 6 and 16, partially overlapping with those of hardwood combustion. The relative abundance of levoglucosan, galactosan and mannosan in smoke also depends on combustion conditions (smouldering or flaming). Therefore, trying to differentiate the type of substrate based solely on the proportions between anhydrosugars remains challenging (Bhattarai et al., 2019; Zhu et al., 2015).

The levoglucosan/OC ratio has also been used to compare different types of biofuels. Alves et al. (2011) obtained a mean value of 13.4 mg levoglucosan g^{-1} OC in samples from a wildfire in Portugal. The levoglucosan/OC ratios for PM_{10} samples from open burning of vine (39 mg g^{-1}), olive (39 mg g^{-1}), acacia (57 mg g^{-1}) and willow (51 mg g^{-1}) branches obtained in a previous study (Alves et al., 2019) were higher than those calculated in this work (8.2–34.2 mg g^{-1}).

After sugars, acids constituted the second most abundant group among the organic compounds analysed. This group comprised n-alkanoic, n-alkanedioic, alkenoic and other types of acids. The homologous series of n-alkanoic acids, from C_8 to C_{31}, presented a clear dominance of even carbon numbers, of which palmitic acid clearly stood out. This acid was also the most abundant chromatographically resolved compound in particulate matter samples from the combustion of bamboo leaves and twigs, sugar cane bagasse and forest litter (Abas et al., 2004). Among acids, those with two carboxylic functional groups were prominent, both in the flaming and smouldering phases, regardless of the type of biofuels

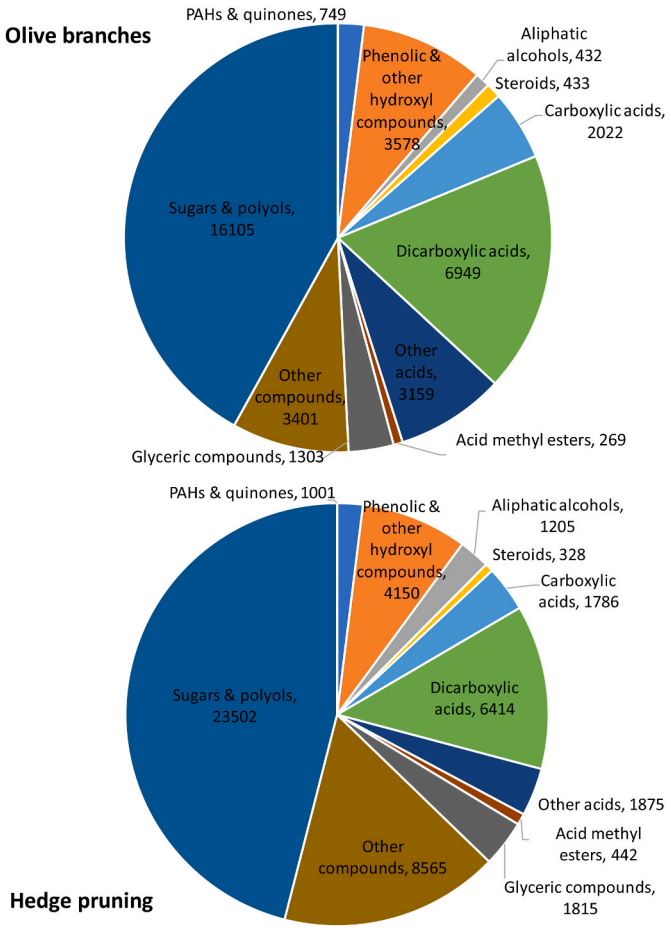

Fig. 1. Organic compounds detected in PM_{10} samples (in μg g^{-1}) from the open burning of olive branches and hedge trimming wastes.

burned. As previously observed in the open burning of tree pruning wastes (Alves et al., 2019), succinic was the most abundant diacid. A significant enhancement in the concentrations of this and other diacids was documented for a biomass burning period in a rural site of Northeast China (Cao et al., 2017). Given their high solubility in water and other physicochemical characteristics, diacids participate in the activation of cloud condensation nuclei and influence the hygroscopic growth of particles. Thus, they represent a significant share of the global aerosol budget and are indirect (cloud-mediated) climate drivers (Yu, 2000).

3-Hydroxypropionic acid, also known as hydracrylic acid, was detected in PM_{10} from burning olive branches at mass fractions 20 times higher than those observed in smoke from hedge trimming waste, presenting substantially higher values in the flaming phase. In contrast, 2-hydroxypropane-1,2,3-tricarboxylic acid (citric acid) was twice as abundant in smoke from hedge branches, showing a significant increase in the smouldering phase. While oleic acid was present in similar amounts in samples from the burning of the various biofuels, linoleic acid was only detected in PM_{10} from hedgerow waste.

Several fatty acid methyl esters (FAME) were found in the samples. The overall amounts emitted were about 2 times higher for hedge trimming waste burning. Palmitic acid methyl ester represented, on average, 26% and 22% of the global emissions of this group of compounds in olive branch combustion and hedge waste samples, respectively. The presence of FAME had previously been observed in particulate matter from a forest fire (Alves et al., 2011), residential biomass combustion (Fine et al., 2004) and prescribed burnings on a shrubland (Alves et al., 2010). Glycerol and esters of glycerol and both palmitic and stearic acids (monopalmitin and monostearin) were also present in PM_{10}. Animal fat mostly consists of triglycerides, which are

esters derived from glycerol combined with three fatty acids. During the cooking process, triglycerides undergo hydrolysis or thermal oxidation, emitting free fatty acids and glycerol (Nolte et al., 1999). However, the detection of this type of compounds in biomass burning smoke indicate that they cannot be used as unique biomarkers of emissions from meat cooking and that other processes, not yet clarified, lead to their production during the combustion of woody and herbaceous material.

Several phenolic compounds, known to be copious in biomass burning emissions (Vicente and Alves, 2018), were observed in the samples, with pyrocatechol (1,2-dihydroxybenzene), tyrosol (4-hydroxyphenylethanol), homoveratryl alcohol (3,4-dimethoxyphenethyl alcohol), resorcinol (3-hydroxyphenol), syringol (2,6-dimethoxyphenol), syringaldehyde (4-hydroxy-3,5-dimethoxybenzaldehyde), syringic acid (4-hydroxy-3,5-dimethoxybenzoic acid) and vanillic acid (4-hydroxy-3-methoxybenzoic acid) being noteworthy due to their abundances. As the burned species belong mainly to the angiosperm group, these phenolics result from the thermal degradation of syringyl and vanillyl lignols that are part of the lignin constitution of this type of plants.

An organophosphate ester, tris(2,4-di-tert-butylphenyl)phosphate (I168O), was observed in substantial amounts (on average, 2198 and 8100 μg g^{-1} PM_{10} for olive branches and hedge trimming wastes, respectively). Acute exposure to this compound has been shown to elicit cardiotoxicity in zebrafish (Zhang et al., 2024). It has been formerly detected in $PM_{2.5}$ samples from 2 Chinese cities (Shi et al., 2020). The authors described it as an widespread component probably resulting from the photodegradation of the antioxidant Irgafos 168 [tris(2,4-di-*tert*-butylphenyl)phosphite] commonly added as ingredient in plastics or from the burning of plasticware, although an origin in pesticides and flame retardants was not ruled out.

Although they did not represent the most abundant group, polycyclic aromatic hydrocarbons (PAHs) are among the most important constituents from the point of view of health effects, given their mutagenic and carcinogenic potential (Kim et al., 2013). Benzo[a]pyrene (B[a]P) is often used as a surrogate marker to assess cancer risks from exposure to complex mixtures (WHO, 2021). In the present work, mass concentrations of B[a]P measured in smoke samples were between 2.7 and 16.4 μg g^{-1}, very similar to those obtained by Sengupta et al. (2023) in laboratory tests with various types of biofuels (2–13 μg g^{-1}). Alves et al. (2019) reported PM_{10} mean mass fractions ranging from 6.51 μg g^{-1} (acacia) to 32.6 μg g^{-1} (olive) for the combustion in the field of wastes from tree pruning. Retene, a substituted PAH mainly emitted from biomass combustion (Scaramboni et al., 2023), is not part of the list of 16 priority PAHs, but has been employed as a biomarker of thermal degradation of abietic acid present in coniferous resin (Ramdahl, 1983). Recently, it has been shown that retene is involved in genotoxicity, oxidative stress, mutagenicity, and cell death (Oliveira Alves et al., 2017; Scaramboni et al., 2023; Vicente et al., 2021). In this study, retene was the dominant PAH, averaging 290 and 339 μg g^{-1} in PM_{10} from the combustion of olive branches and hedge pruning wastes, respectively. It was observed that its emissions were higher during the smouldering phase. 2,6-Di-tert-butyl-1,4-benzoquinone was co-emitted with PAHs. On average, this quinone accounted for 193 and 422 μg g^{-1} of PM_{10} from the burning of olive branches and hedge trimming waste, reaching a peak of 1260 μg g^{-1} during the smouldering phase of this last biofuel.

3.3. Oxidative potential (OP)

Mass-normalised OP values for both assays are shown in Table 6. The values of this study were higher than those found in ambient air in other areas of Europe, such as the rural site of Novaledo (Northern Italy), despite being heavily influenced by residential wood burning (DTT = 0.011 nmol min^{-1} μg^{-1} and AA = 0.009 nmol min^{-1} μg^{-1}; Pietrogrande et al., 2021).

DTT activities were very similar to those reported by Fushimi et al. (2017) in an open burning experiment of crop residues in Japan (0.009–0.030 nmol min^{-1} μg^{-1}) and by Verma et al. (2009) in forest fire smoke in California (0.023–0.13 nmol min^{-1} μg^{-1}). In contrast, Jin et al. (2016) obtained higher values for wood and straw combustion in China (0.06 and 0.08 nmol min^{-1} μg^{-1}, respectively), while lower DTT activities were obtained by Li et al. (2019) and Zhu et al. (2019) in combustion experiments using biomass (0.0014 nmol min^{-1} μg^{-1}), coal (0.0021 nmol min^{-1} μg^{-1}) and diesel (0.0023 nmol min^{-1} μg^{-1}). To the best of our knowledge, no previous works on the oxidative potential on PM samples under the influence of biomass open burning have been performed.

Table 6
OP values for the AA and DTT assays (in nmol min^{-1} μg^{-1}).

	OP^{AA}	OP^{DTT}
AL-2	0.009	0.010
AL-3	0.032	0.020
AL-4	0.030	0.030
AL-5	0.019	0.016
AL-6	0.047	0.049

3.4. Cytotoxicity and EC_{50}

Organic extracts of PM_{10} samples collected from open burning of olive branches and hedge trimming residues showed an effect on the metabolic activity of A549 cells. The results of the lung cell culture cytotoxicity assays are shown in Fig. 2. In these tests, cell viability was measured at different doses of the aerosol collected for each sample. As can be seen, viability decreased as the exposure dose increased. Statistically significant differences between samples were observed for the highest doses (50, 100 and 200 μg ml^{-1}). A previous study on PM_{10} emitted during crop residue burning in Portugal also showed dose-dependent cytotoxicity (Vicente et al., 2022).

The results from the MTT assays were used to create dose–response curves and to determine the EC_{50} for PM_{10} (concentration required to decrease cell viability by 50%). EC_{50} values of 167, 119, 103, 110 and 94 μg ml^{-1} were obtained for samples AL-2, AL-3, AL-4, AL-5 and AL-6, respectively. In a previous study carried out in the same region (Vicente et al., 2022), EC_{50} values from 9.6 to 13.3 μg ml^{-1} were achieved for the different combustion stages of olive branches. The differences may be attributed to the use of different bioassays to evaluate cytotoxicity in the previous study (water-soluble tetrazolium, WST-8, and lactate dehydrogenase, LDH). Although all these assays are colorimetric, they are based on distinct mechanisms: LDH evaluates cell membrane integrity, while WST-8 and MTT assess mitochondrial activity (Vicente et al., 2024). Results have been reported to be strongly assay-dependent (Braun et al., 2018; Vicente et al., 2021), even between WST-8 and MTT (Braun et al., 2018). Additionally, several studies have indicated that the toxicity of particulate matter is influenced by its chemical

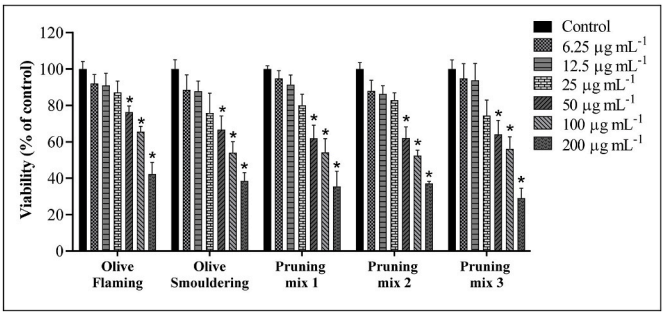

Fig. 2. Cell viability assessed with the MTT assay after 24 h exposure to increasing PM_{10} concentrations: control, 6.25, 12.5, 25, 50, 100 and 200 μg ml^{-1}. Bars represent mean ± SD. Asterisks indicate statistical significance compared to the respective control (n = 10, $p < 0.05$).

composition (Chuang et al., 2019; Nemmar et al., 2013; Peixoto et al., 2017; Schwarze et al., 2006; Wang et al., 2020). Concerning agricultural burning, this composition is determined by several factors, including the type of fuel used, the burning method (e.g., spread vs. pile residues), water content, combustion phase, and environmental conditions (Gonçalves et al., 2011; Hayashi et al., 2014; Kim Oanh et al., 2011; Zhang et al., 2013).

3.5. Relationships between biological responses and PM_{10} chemical constituents

The supplementary material includes the results of Spearman's bivariate correlations between toxicity assays and PM_{10} chemical components (Tables S3 and S4). The intrinsic oxidative potential was correlated against the mass fraction of chemical components, while EC_{50} values were correlated against concentrations per unit volume.

Positive correlations were found between EC_{50} and organic components (OC and WSOC), which is in agreement with previous works showing that carbonaceous compounds have adverse effects on human health (Molina et al., 2020). Other studies also concluded that WSOC significantly contributes to cytotoxicity (e.g., Ge et al., 2023; Wang et al., 2018). Significant positive correlations between EC_{50} and several PAHs, galactosan and phenolic compounds usually described as biomass burning markers (Vicente and Alves, 2018) were also found. Among these relationships, that of retene stands out (p-value<0.01). Tavangar et al. (2024) also reported significant correlations between cytotoxicity and some PAHs, including retene. Oliveira Alves et al. (2017) exposed human lung cells to PM_{10} from biomass burning in the Amazon region and concluded that retene induces DNA damage and cell death, mainly by necrosis. Since retene is not on the list of 16 priority PAHs of the United States Environmental Protection Agency, it is necessary to encourage further studies that prove its possible carcinogenicity for eventual inclusion in the future. Using airway epithelial cells, Van Den Heuvel et al. (2018) evaluated the toxicity of PM_{10} and its relationship with tracers of biomass burning. Reduced cell viability and induction of interleukin-8 (an indicator of inflammatory potency) were associated with all markers for this emission source. The researchers argued that biomass burning tracers, such as anhydrosugars, are not considered toxic as they are rapidly excreted unchanged in urine. Thus, toxic effects cannot be assigned to themselves, but rather to other co-emitted components. Although the cellular mechanisms of toxicity are not fully understood, it is known that exposure to PM-bound constituents from biomass burning trigger an overproduction of reactive oxygen species (ROS) and reactive nitrogen species (RNS). These reactive species damage cellular physiological and biochemical processes by mechanisms that induce oxidative stress, release of inflammatory mediators such as tumor necrosis factors (TNF) and interleukins (IL), and genotoxicity, followed by programmed cell death pathways (Vicente et al., 2024).

In line with what was observed in other works (Besis et al., 2023; Yu et al., 2022), WSOC also showed a significant positive correlation with DTT. Good correlations were also found between OP^{DTT} values and some PAHs, as reported by other authors (Pietrogrande et al., 2021). Although PAHs are not considered DTT active (Wong et al., 2019), their relationship with the DTT assay may be explained by the fact that they are released into the atmosphere along with redox-active quinones by biomass combustion (van Drooge and Grimalt, 2015). Some organic compounds, such as quinones and PAHs, can generate superoxide radicals, which are precursors of Fenton reactions and generate more reactive radicals like $OH^{\bullet}$ with a great impact on PM toxicity (Raparthi et al., 2023, and references therein). As observed in the MTT assay, some phenolic compounds showed positive and significant relationships with OP^{DTT}. These include compounds from the methoxyphenol family, such as syringic acid and 2-methoxy-4-propylphenol, also known as 4-propylguaicol. A strong correlation between methoxyphenols and OP^{DTT} was also reported for PM_{10} collected in Chamonix, a French city heavily impacted in winter by biomass burning (Calas et al., 2018).

The AA assay is usually sensitive to transition metals such as Cu and Fe (Bates et al., 2019). In this work, positive correlations with Ti, Mn, Fe and Ni were found. A relationship between OP^{AA} and these metals was also reported in previous studies (Expósito et al., 2024; Kim et al., 2024; Pietrogrande et al., 2021). Some species were inversely correlated with OP^{AA}, which may be due to their lower redox properties. Furthermore, these properties can be significantly altered because of both synergistic and antagonistic interactions between PM components (Gao et al., 2020).

4. Conclusions

This study provided emission factors for gaseous pollutants (CO_2, CO, N_2O, NO_2, HCl, HF, CH_4, C_2H_6, C_2H_4, C_3H_8, C_6H_{14}, CHOH), chemical speciation of organic and inorganic components of PM_{10} (EC, OC, WSOC, metals, water soluble ions, and more than 120 other organic compounds), as well as an assessment of the oxidative potential and cellular cytotoxicity of the particulate material emitted during the backyard burning of olive tree pruning branches and hedge trimming waste mixtures. In general, the EFs of green waste combustion obtained in the present study agree well with the few data available in the literature. In addition to conventional combustion gases (CO_2 and CO), significant emissions of methane, formaldehyde and other gases were observed. PM_{10} was dominated by organic carbon, 50% of which was found to be water soluble. Soluble ions accounted for up to 21% of the PM_{10} mass. The most abundant ions were Cl^-, K^+ and SO_4^{2-}, while most elements were detected at trace levels. The most abundant PAH found in the samples was retene. Levoglucosan, mannosan and galactosan were among the most abundant organic compounds.

The results indicated that the combustion phase and the type of biomass residue can have a significant effect on the toxicological properties of the emitted PM_{10}. All samples significantly reduced the viability of alveolar epithelial cells. Cell viability decreased with increasing doses of PM_{10}. PM_{10} also caused an increase in OP (126–133 nmol min^{-1} m^{-3}). WSOC, several PAH, some phenolic compounds and a few acids correlated with cell viability and OP.

The results suggest the need to draw the attention of the authorities to the possible impact of particulate matter on human health, stricter regulations and the search for environmentally safer alternatives. Given that open burning of pruning and garden waste emits a wide range of atmospheric pollutants, including short-lived climate forcers and toxic particulate matter constituents with deleterious health effects, through legal action, this type of burning must be restricted or outright banned. Composting, shredding and biochar production are a few effective sustainable techniques that can help to curtail the issue while also helping to retain nutrients and moisture in the soil. However, given the limited and sporadic production of residual biomass by farmers and gardeners, these solutions are only viable if they are made available by municipal services, as is already the case in some locations. Along with technical solutions, active stakeholder involvement, including education, awareness and empowerment of residual biomass producers, are also needed to change ways of thinking and acting.

This comprehensive study can also contribute to improving emission inventories and feeding the SPECIEUROPE database, thus helping in the application of source apportionment models. However, given that emissions and their chemical signatures depend on numerous factors, including the type of biofuels, and their elemental composition and ash content, it is desirable to promote new studies to complement the existing information.

CRediT authorship contribution statement

A. López-Caravaca: Writing – review & editing, Writing – original draft, Investigation, Formal analysis. **E.D. Vicente:** Writing – review & editing, Investigation, Formal analysis. **D. Figueiredo:** Writing – review

& editing, Investigation. **M. Evtyugina:** Writing – review & editing, Investigation. **J.F. Nicolás:** Writing – review & editing, Investigation. **E. Yubero:** Writing – review & editing, Resources, Investigation. **N. Galindo:** Writing – review & editing, Writing – original draft, Validation, Supervision, Resources, Funding acquisition, Formal analysis. **Jiří Ryšavý:** Writing – review & editing, Resources, Funding acquisition, Formal analysis. **C.A. Alves:** Writing – review & editing, Writing – original draft, Validation, Supervision, Resources, Project administration, Funding acquisition, Formal analysis, Conceptualization.

Declaration of competing interest

The authors declare no conflict of interest.

Data availability

Data will be made available on request.

Acknowledgements

The chemical characterisation and cytotoxic evaluation of PM_{10} samples was partially funded by the Portuguese Foundation for Science and Technology (FCT) through the project "Air Pollution in an African Megacity: Source Apportionment and Health Implications" – APAM (DOI: 10.54499/2022.04240.PTDC), financially supported by national funds (OE), through FCT/MCTES. The work was also financially supported by the European Union under the REFRESH – Research Excellence for Region Sustainability and High-tech Industries project No. CZ.10.03.01/00/22_003/0000048 via the Operational Programme Just Transition. The financial support to CESAM by FCT/MCTES (UIDP/50017/2020 + UIDB/50017/2020 + LA/P/0094/2020), through national funds, is also acknowledged. FCT is also acknowledged for the research contract under Scientific Employment Stimulus to Estela D. Vicente (CEECIND/00399/2022) and for the PhD fellowship 2020.06414.BD to Daniela Figueiredo. A. López-Caravaca thanks the Spanish Ministry of Science and Innovation for a predoctoral grant (PRE2019-089098).

Appendix A. Supplementary data

Supplementary data to this article can be found online at https://doi.org/10.1016/j.atmosenv.2024.120849.

References

Abas, M.R., Oros, D.R., Simoneit, B.R.T., 2004. Biomass burning as the main source of organic aerosol particulate matter in Malaysia during haze episodes. Chemosphere 55, 1089–1095.

Akagi, S.K., Yokelson, R.J., Wiedinmyer, C., Alvarado, M.J., Reid, J.S., Karl, T., Crounse, J.D., Wennberg, P.O., 2011. Emission factors for open and domestic biomass burning for use in atmospheric models. Atmos. Chem. Phys. 11, 4039–4072.

Akbari, M.Z., Thepnuan, D., Wiriya, W., Janta, R., Punsompong, P., Hemwan, P., Charoenpanyanet, A., Chantara, S., 2021. Emission factors of metals bound with $PM_{2.5}$ and ashes from biomass burning simulated in an open-system combustion chamber for estimation of open burning emissions. Atmos. Pollut. Res. 12, 13–24.

Alves, C.A., Gonçalves, C., Pio, C.A., Mirante, F., Caseiro, A., Tarelho, L., Freitas, M.C., Viegas, D.X., 2010. Smoke emissions from biomass burning in a Mediterranean shrubland. Atmos. Environ. 44, 3024–3033.

Alves, C.A., Vicente, A., Monteiro, C., Gonçalves, C., Evtyugina, M., Pio, C., 2011. Emission of trace gases and organic components in smoke particles from a wildfire in a mixed-evergreen forest in Portugal. Sci. Total Environ. 409, 1466–1475.

Alves, C.A., Vicente, E.D., Evtyugina, M., Vicente, A., Pio, C., Fernández Amado, M., López Mahía, P., 2019. Gaseous and speciated particulate emissions from the open burning of wastes from tree pruning. Atmos. Res. 226, 110–121.

Andreae, M.O., 2019. Emission of trace gases and aerosols from biomass burning – an updated assessment. Atmos. Chem. Phys. 19, 8523–8546.

Bates, J.T., Fang, T., Verma, V., Zeng, L., Weber, R.J., Tolbert, P.E., Abrams, J.Y., Sarnat, S.E., Klein, M., Mulholland, J.A., Russel, A.G., 2019. Review of acellular assays of ambient particulate matter oxidative potential: methods and relationships with composition, sources, and health effects. Environ. Sci. Technol. 53, 4003–4019.

Besis, A., Romano, M.P., Serafeim, E., Avgenikou, A., Kouras, A., Lionetto, M.G., Guascito, M.R., De Bartolomeo, A.R., Giordano, M.E., Mangone, A., Contini, D., Samara, C., 2023. Size-resolved redox activity and cytotoxicity of water-soluble urban atmospheric particulate matter: assessing contributions from chemical components. Toxics 11, 59.

Bhattarai, H., Saikawa, E., Wan, X., Zhu, H., Ram, K., Gao, S., Kang, S., Zhang, Q., Zhang, Y., Wu, G., Wang, X., Kawamura, K., Fu, P., Cong, Z., 2019. Levoglucosan as a tracer of biomass burning: recent progress and perspectives. Atmos. Res. 220, 20–33.

Boreddy, S.K.R., Mozammel Haque, M., Kawamura, K., 2018. Long- term (2001– 2012) trends of carbonaceous aerosols from a remote island in the Western North Pacific: an outflow region of Asian pollutants. Atmos. Chem. Phys. 18, 1291–1306.

Braun, K., Stürzel, C.M., Biskupek, J., Kaiser, U., Kirchhoff, F., Lindén, M., 2018. Comparison of different cytotoxicity assays for *in vitro* evaluation of mesoporous silica nanoparticles. Toxicol. in Vitro 52, 214–221.

Cao, F., Zhang, S.-C., Kawamura, K., Liu, X., Yang, C., Xu, Z., Fan, M., Zhang, W., Bao, M., Chang, Y., Song, W., Liu, S., Lee, X., Li, J., Zhang, G., Zhang, Y.-L., 2017. Chemical characteristics of dicarboxylic acids and related organic compounds in $PM_{2.5}$ during biomass-burning and non-biomass-burning seasons at a rural site of Northeast China. Environ. Pollut. 231, 654–662.

Calas, A., Uzu, G., Kelly, F.J., Houdier, S., Martins, J.M.F., Thomas, F., Molton, F., Charron, A., Dunster, C., Oliete, A., Jacob, V., Besombes, J.L., Chevrier, F., Jaffrezo, J.L., 2018. Comparison between five acellular oxidative potential measurement assays performed with detailed chemistry on PM_{10} samples from the city of Chamonix (France). Atmos. Chem. Phys. 18, 7863–7875.

Chantara, S., Thepnuan, D., Wiriya, W., Prawan, S., Tsai, Y.I., 2019. Emissions of pollutant gases, fine particulate matters and their significant tracers from biomass burning in an open-system combustion chamber. Chemosphere 224, 407–416.

Chen, H., 2014. Chemical composition and structure of natural lignocellulose. In: Biotechnology of Lignocellulose. Springer, Dordrecht.

Chen, J., Li, C., Ristovski, Z., Milic, A., Gu, Y., Islam, M.S., Wang, S., Hao, J., Zhang, H., He, C., Guo, H., Fu, H., Miljevic, B., Morawska, L., Thai, P., Lam, Y.F., Pereira, G., Ding, A., Huang, X., Dumka, U.C., 2017. A review of biomass burning: emissions and impacts on air quality, health and climate in China. Sci. Total Environ. 579, 1000–1034.

Cheung, K.L., Polidori, A., Ntziachristos, L., Tzamkiozis, T., Samaras, Z., Cassee, F.R., Gerlofs, M., Sioutas, C., 2009. Chemical characteristics and oxidative potential of particulate matter emissions from gasoline, diesel, and biodiesel cars. Environ. Sci. Technol. 43, 6334–6340.

Chiari, M., Yubero, Y., Calzolai, G., Lucarelli, F., Crespo, J., Galindo, N., Nicolás, J.F., Giannoni, M., Nava, S., 2018. Comparison of PIXE and XRF analysis of airborne particulate matter samples collected on Teflon and quartz fibre filters. Nucl. Instrum. Methods B 417, 128–132.

Chuang, H.C., Sun, J., Ni, H., Tian, J., Lui, K.H., Han, Y., Cao, J., Huang, R.J., Shen, Z., Ho, K.F., 2019. Characterization of the chemical components and bioreactivity of fine particulate matter produced during crop-residue burning in China. Environ. Pollut. 245, 226–234.

Clemente, Á., Gil-Moltó, J., Yubero, E., Juárez, N., Nicolás, J.F., Crespo, J., Galindo, N., 2023. Sensitivity of PM_{10} oxidative potential to aerosol chemical composition at a Mediterranean urban site: ascorbic acid versus dithiothreitol measurements. Air Qual. Atmos. Health 16, 1165–1172.

Comite, V., Miani, A., Ricca, M., La Russa, M., Pulimeno, M., Fermo, P., 2021. The impact of atmospheric pollution on outdoor cultural heritage: an analytic methodology for the characterization of the carbonaceous fraction in black crusts present on stone surfaces. Environ. Res. 201, 111565.

Das, R., Wang, X., Itoh, M., Shiodera, S., Kuwata, M., 2019. Estimation of metal emissions from tropical peatland burning in Indonesia by controlled laboratory experiments. J. Geophys. Res. Atmos. 124, 6583–6599.

Deshpande, M.V., Kumar, N., Pillai, D., Krishna, V.V., Jain, M., 2023. Greenhouse gas emissions from agricultural residue burning have increased by 75 % since 2011 across India. Sci. Total Environ. 904, 166944.

Desservettaz, M., Pikridas, M., Stavroulas, I., Bougiatioti, A., Liakakou, E., Hatzianastassiou, N., Sciare, J., Mihalopoulos, N., Bourtsoukidis, E., 2023. Emission of volatile organic compounds from residential biomass burning and their rapid chemical transformations. Sci. Total Environ. 903, 166592.

Engling, G., Carrico, C.M., Kreidenweis, S.M., Collett Jr., J.L., Day, D.E., Malm, W.C., Hao, W.M., Lincoln, E., Iinuma, Y., Herrmann, H., 2006. Determination of levoglucosan in biomass combustion aerosol by high performance anion exchange chromatography with pulsed amperometric detection. Atmos. Environ. 40, S299–S311.

Engling, G., Lee, J.J., Tsai, Y.-W., Lung, S.-C.C., Chou, C.C.-K., Chan, C.-Y., 2009. Size-resolved anhydrosugar composition in smoke aerosol from controlled field burning of rice straw. Aerosol Sci. Technol. 43, 662–672.

Expósito, A., Markiv, B., Santibáñez, M., Fadel, M., Ledoux, F., Courcot, D., Fernández-Olmo, I., 2024. Ascorbate oxidation driven by $PM_{2.5}$-bound metal(loid)s extracted in an acidic simulated lung fluid in relation to their bioaccessibility. Air Qual. Atmos. Health 17, 177–189.

Fine, P.M., Cass, G.R., Simoneit, B.R., 2001. Chemical characterization of fine particle emissions from fireplace combustion of woods grown in the northeastern United States. Environ. Sci. Technol. 35, 2665–2675.

Fine, P.M., Cass, G.R., Simoneit, B.R.T., 2004. Chemical characterization of fine particle emissions from the fireplace combustion of wood types grown in the midwestern and western United States. Environ. Eng. Sci. 21, 387–409.

Fushimi, A., Saitoh, K., Hayashi, K., Ono, K., Fujitani, Y., Villalobos, A.M., Shelton, B.R., Takami, A., Tanabe, K., Schauer, J.J., 2017. Chemical characterization and oxidative potential of particles emitted from open burning of cereal straws and rice husk under flaming and smoldering conditions. Atmos. Environ. 163, 118–127.

Gao, D., Ripley, S., Weichenthal, S., Godri Pollitt, K.J., 2020. Ambient particulate matter oxidative potential: chemical determinants, associated health effects, and strategies for risk management. Free Radic. Biol. Med. 151, 7–25.
Ge, P., Liu, Z., Chen, M., Cui, Y., Cao, M., Liu, X., 2023. Chemical characteristics and cytotoxicity to GC-2spd(ts) cells of $PM_{2.5}$ in Nanjing Jiangbei new area from 2015 to 2019. Toxics 11, 92.
Gonçalves, C., Evtyugina, M., Alves, C., Monteiro, C., Pio, C., Tomé, M., 2011. Organic particulate emissions from field burning of garden and agriculture residues. Atmos. Res. 101, 666–680.
Gonçalves, C., Rienda, I.C., Pina, N., Gama, C., Nunes, T., Tchepel, O., Alves, C., 2021. PM_{10}-bound sugars: chemical composition, sources and seasonal variations. Atmosphere 12, 194.
Graham, B., Mayol-Bracero, O.L., Guyon, P., Roberts, G.C., Decesari, S., Facchini, M.C., Artaxo, P., Maenhaut, W., Koll, P., Andreae, M.O., 2002. Water soluble organic compounds in biomass burning aerosols over Amazonia 1. Characterization by NMR and GC-MS. J. Geophys. Res. 107, 8047.
Hayashi, K., Ono, K., Kajiura, M., Sudo, S., Yonemura, S., Fushimi, A., Saitoh, K., Fujitani, Y., Tanabe, K., 2014. Trace gas and particle emissions from open burning of three cereal crop residues: increase in residue moistness enhances emissions of carbon monoxide, methane, and particulate organic carbon. Atmos. Environ. 95, 36–44.
Jiang, K., Xing, R., Luo, Z., Huang, W., Yi, F., Men, Y., Zhao, N., Chang, Z., Zhao, J., Pan, B., Shen, G., 2024. Pollutant emissions from biomass burning: a review on emission characteristics, environmental impacts, and research perspectives. Particuology 85, 296–309.
Jin, W., Su, S., Wang, B., Zhu, X., Chen, Y., Shen, G., Liu, J., Cheng, H., Wang, X., Wu, S., Zeng, E., Xing, B., Tao, S., 2016. Properties and cellular effects of particulate matter from direct emissions and ambient sources. J. Environ. Sci. Health. A 51, 1075–1083.
Jing, B., Peng, C., Wang, Y., Liu, Q., Tong, S., Zhang, Y., Ge, M., 2017. Hygroscopic properties of potassium chloride and its internal mixtures with organic compounds relevant to biomass burning aerosol particles. Sci. Rep. 7, 43572.
Johnston, H.J., Mueller, W., Steinle, S., Vardoulakis, S., Tantrakarnapa, K., Loh, M., Cherrie, J.W., 2019. How harmful is particulate matter emitted from biomass burning? A Thailand perspective. Curr. Pollut. Rep. 5, 353–377.
Karanasiou, A., Alastuey, A., Amato, F., Renzi, M., Stafoggia, M., Tobias, A., Reche, C., Forastiere, F., Gumy, S., Mudu, P., Querol, X., 2021. Short-term health effects from outdoor exposure to biomass burning emissions: a review. Sci. Total Environ. 781, 146739.
Keywood, M., Kanakidou, M., Stohl, A., Dentener, F., Grassi, G., Meyer, C.P., Torseth, K., Edwards, D., Thompson, A.M., Lohmann, U., Burrows, J., 2013. Fire in the air: biomass burning impacts in a changing climate. Crit. Rev. Environ. Sci. Technol. 43, 40–83.
Kim Oanh, N.T., Ly, B.T., Tipayarom, D., Manandhar, B.R., Prapat, P., Simpson, C.D., Sally Liu, L.J., 2011. Characterization of particulate matter emission from open burning of rice straw. Atmos. Environ. 45, 493–502.
Kim, K.H., Jahan, S.A., Kabir, E., Brown, R.J.C., 2013. A review of airborne polycyclic aromatic hydrocarbons (PAHs) and their human health effects. Environ. Int. 60, 71–80.
Kim, P.R., Park, S.W., Han, Y.J., Lee, M.H., Holsen, T.M., Jeong, C.H., Evans, G., 2024. Variations of oxidative potential of $PM_{2.5}$ in a medium-sized residential city in South Korea measured using three different chemical assays. Sci. Total Environ. 920, 171053.
Kondo, Y., Miyazaki, Y., Takegawa, N., Miyakawa, T., Weber, R.J., Jimenez, J.L., Zhang, Q., Worsnop, D.R., 2007. Oxygenated and water-soluble organic aerosols in Tokyo. J. Geophys. Res. 112, D01203.
Koppmann, R., von Czapiewski, K., Reid, J.S., 2005. A review of biomass burning emissions, part I: gaseous emissions of carbon monoxide, methane, volatile organic compounds, and nitrogen containing compounds. Atmos. Chem. Phys. Discuss. 5, 10455–10516.
Lacey, R.E., Faulker, W.B., 2015. Uncertainty associated with the gravimetric measurement of particulate matter concentration in ambient air. J. Air Waste Manag. Assoc. 65, 887–894.
Lelieveld, J., Klingmüller, K., Pozzer, A., Burnett, R.T., Haines, A., Ramanathan, V., 2019. Effects of fossil fuel and total anthropogenic emission removal on public health and climate. Proc. Natl. Acad. Sci. 116, 7192–7197.
Li, R., Han, Y., Wang, L., Shang, Y., Chen, Y., 2019. Differences in oxidative potential of black carbon from three combustion emission sources in China. J. Environ. Manage. 240, 57–65.
Li, W., Ge, P., Chen, M., Tang, J., Cao, M., Cui, Y., Hu, K., Nie, D., 2021. Tracers from biomass burning emissions and identification of biomass burning. Atmosphere 12, 1401.
Ma, S., He, F., Tian, D., Zou, D., Yan, Z., Yang, Y., Zhou, T., Huang, K., Shen, H., Fang, J., 2018. Variations and determinants of carbon content in plants: a global synthesis. Biogeosciences 15, 693–702.
Mayol-Bracero, O.L., Guyon, P., Graham, B., Roberts, G., Andreae, M.O., Decesari, S., Facchini, M.C., Fuzzi, S., Artaxo, P., 2002. Water-soluble organic compounds in biomass burning aerosols over Amazonia 2. Apportionment of the chemical composition and importance of the polyacidic fraction. J. Geophys. Res. 107, 8091.
Molina, C., Toro, R., Manzano, C.A., Canepari, S., Massimi, L., Leiva-Guzmám, M.A., 2020. Airborne aerosols and human health: leapfrogging from mass concentration to oxidative potential. Atmosphere 11, 917.
Mugica-Álvarez, V., Hernández-Rosas, F., Magaña-Reyes, M., Herrera-Murillo, J., Santiago de la Rosa, N., Gutiérrez-Arzaluz, M., Figueroa-Lara, J.J., González-Cardoso, G., 2018. Sugarcane burning emissions: characterization and emission factors. Atmos. Environ. 193, 262–272.
Nemmar, A., Holme, J.A., Rosas, I., Schwarze, P.E., Alfaro-Moreno, E., 2013. Recent advances in particulate matter and nanoparticle toxicology: a review of the *in vivo* and *in vitro* studies. BioMed Res. Int. 2013.
Ni, H., Tian, J., Wang, X., Wang, Q., Han, Y., Cao, J., Long, X., Chen, L.W.A., Chow, J.C., Watson, J.W., Huang, R.J., Dusek, U., 2017. $PM_{2.5}$ emissions and source profiles from open burning of crop residues. Atmos. Environ. 169, 229–237.
Nolte, C.G., Schauer, J.J., Cass, G.R., Simoneit, B.R.T., 1999. Highly polar organic compounds present in meat smoke. Environ. Sci. Technol. 33, 3313–3316.
Oanh, N.T.K., Ly, B.T., Tipayarom, D., Manandhar, B.R., Prapat, P., Simpson, C.D., Sally Liu, L.-J., 2011. Characterization of particulate matter emission from open burning of rice straw. Atmos. Environ. 45, 493–502.
Oliveira Alves, N., Vessoni, A.T., Quinet, A., Fortunato, R.S., Kajitani, G.S., Peixoto, M.S., de Souza, S., Artaxo, P., Saldiva, P., Martins, C.F., Batistuzzo, S.R., 2017. Biomass burning in the Amazon region causes DNA damage and cell death in human lung cells. Sci. Rep. 7, 10937.
Pani, S.K., Chantara, S., Khamkaew, C., Lee, C.T., Lin, N.H., 2019. Biomass burning in the northern peninsular Southeast Asia: aerosol chemical profile and potential exposure. Atmos. Res. 224, 180–195.
Peixoto, M.S., de Oliveira Galvão, M.F., Batistuzzo de Medeiros, S.R., 2017. Cell death pathways of particulate matter toxicity. Chemosphere 188, 32–48.
Pernigotti, D., Belis, C.A., Spanò, L., 2016. SPECIEUROPE: the European data base for PM source profiles. Atmos. Pollut. Res. 7, 307–314.
Pietrogrande, M.C., Bertoli, I., Clauser, G., Dalpiaz, C., Dell'Anna, R., Lazzeri, P., Lenzi, W., Russo, M., 2021. Chemical composition and oxidative potential of atmospheric particles heavily impacted by residential wood burning in the alpine region of northern Italy. Atmos. Environ. 253, 118360.
Pinto, E., Almeida, A., Ferreira, I.M., 2016. Essential and non-essential/toxic elements in rice available in the Portuguese and Spanish markets. J. Food Compos. Anal. 48, 81–87.
Pio, C., Cerqueira, M., Harrison, R.M., Nunes, T., Mirante, F., Alves, C., Oliveira, C., Sanchez de la Campa, A., Begoña Artíñano, B., Matos, M., 2011. OC/EC ratio observations in Europe: Re-thinking the approach for apportionment between primary and secondary organic carbon. Atmos. Environ. 45, 6121–6132.
Rajput, P., Sarin, M., Kundu, S.S., 2013. Atmospheric particulate matter ($PM_{2.5}$), EC, OC, WSOC and PAHs from NE–Himalaya: abundances and chemical characteristics. Atmos. Pollut. Res. 4, 214–221.
Ramdahl, T., 1983. Retene - a molecular marker of wood combustion in ambient air. Nature 306, 580–582.
Ramya, C.B., Aswini, A.R., Hegde, P., Boreddy, S.-K.R., Babu, S.S., 2023. Water-soluble organic aerosols over South Asia – seasonal changes and source characteristics. Sci. Total Environ. 900, 165644.
Raparthi, N., Yadav, S., Khare, A., Dubey, S., Phuleria, H.C., 2023. Chemical and oxidative properties of fine particulate matter from near-road traffic sources. Environ. Pollut. 337, 122514.
Ravindra, K., Sokhi, R., Van Grieken, R., 2008. Atmospheric polycyclic aromatic hydrocarbons: source attribution, emission factors and regulation. Atmos. Environ. 42, 2895–2921.
Ravindra, K., Singh, T., Mor, S., 2019. Emissions of air pollutants from primary crop residue burning in India and their mitigation strategies for cleaner emissions. J. Cleaner Prod. 208, 261–273.
Reddington, C.L., Morgan, W.T., Darbyshire, E., Brito, J., Coe, H., Artaxo, P., Scott, C.E., Marsham, J., Spracklen, D.V., 2019. Biomass burning aerosol over the Amazon: analysis of aircraft, surface and satellite observations using a global aerosol model. Atmos. Chem. Phys. 19, 9125–9152.
Ren-Jian, Z., Kin-Fai, H., Zhen-Xing, S., 2012. The role of Aerosol in climate change, the environment, and human health. Atmos. Oceanic Sci. Lett. 5, 156–161.
Saarikoski, S., Timonen, H., Saarnio, K., Aurela, M., Jarvi, L., Keronen, P., Kerminen, V. M., Hillamo, R., 2008. Sources of organic carbon in fine particulate matter in northern European urban air. Atmos. Chem. Phys. 8, 6281–6295.
Sahai, S., Sharma, C., Singh, D.P., Dixit, C.K., Singh, N., Sharma, P., Singh, K., Bhatt, S., Ghude, S., Gupta, V., Gupta, R.K., Tiwari, M.K., Garg, S.C., Mitra, A.P., Gupta, P.K., 2007. A study for development of emission factors for trace gases and carbonaceous particulate species from in situ burning of wheat straw in agricultural fields in India. Atmos. Environ. 41, 9173–9186.
Sang, X., Zhang, Z., Chan, C., Engling, G., 2013. Source categories and contribution of biomass smoke to organic aerosol over the southeastern Tibetan plateau. Atmos. Environ. 78, 113–123.
Santiago de la Rosa, N., González-Cardoso, G., Figueroa-Lara, J.J., Gutiérrez-Arzaluz, M., Octaviano-Villasana, C., Ramírez-Hernández, I.F., Mugica-Álvarez, V., 2018. Emission factors of atmospheric and climatic pollutants from crop residues burning. J. Air Waste Manag. Assoc. 68, 849–865.
Scaramboni, C., Arruda Moura Campos, M.L., Junqueira Dorta, D., Palma de Oliveira, D., Regina Batistuzzo de Medeiros, R., de Oliveira Galvão, M.F., Dreij, K., 2023. Reactive oxygen species-dependent transient induction of genotoxicity by retene in human liver HepG2 cells. Toxicol. Vitro 91, 105628.
Schmidl, C., Luisser, M., Padouvas, E., Lasselsberger, L., Rzaca, M., Ramirez-Santa Cruz, C., Handler, M., Peng, G., Bauer, H., Puxbaum, H., 2011. Particulate and gaseous emissions from manually and automatically fired small scale combustion systems. Atmos. Environ. 45, 7443–7454.
Schwarze, P.E., Øvrevik, J., Lag, M., Refsnes, M., Nafstad, P., Hetland, R., Dybing, E., 2006. Particulate matter properties and health effects: consistency of epidemiological and toxicological studies. Hum. Exp. Toxicol. 25, 559–579.
Sengupta, D., Samburova, V., Bhattarai, C., Moosmüller, H., Khlystov, A., 2023. Emission factors for polycyclic aromatic hydrocarbons from laboratory biomass-burning and their chemical transformations during aging in an oxidation flow reactor. Sci. Total Environ. 870, 161857.

Shi, J., Xu, C., Xiang, L., Chen, J., Cai, Z., 2020. Tris(2,4-di-*tert*-butylphenyl)phosphate: an unexpected abundant toxic pollutant found in $PM_{2.5}$. Environ. Sci. Technol. 54, 10570–10576.

Sigsgaard, T., Forsberg, B., Annesi-Maesano, I., Blomberg, A., Bølling, A., Boman, C., Bønløkke, J., Brauer, M., Bruce, N., Héroux, M.E., Hirvonen, M.R., Kelly, F., Künzli, N., Lundbäck, B., Moshammer, H., Noonan, C., Pagels, J., Sallsten, G., Sculier, J.P., Brunekreef, B., 2015. Health impacts of anthropogenic biomass burning in the developed world. Eur. Respir. J. 46, 1577–1588.

Tavangar, F.Z., Javeri, Z., Nikaeen, M., Sharafi, M., Mohammadi, F., Karimi, H., Nafez, A. H., 2024. Cytotoxicity and genotoxicity of fine particulate matter ($PM_{2.5}$): a polluted city experiencing Middle East dust events. Air Qual. Atmos. Health 17, 789–798.

Thomas, S.C., Martin, A.R., 2012. Carbon content of tree tissues: a synthesis. Forests 3, 332–352.

Tian, J., Ni, H., Cao, J., Han, Y., Wang, Q., Wang, X., Chen, L.W.A., Chow, J.C., Watson, J.G., Wei, C., Sun, J., Zhang, T., Huang, R., 2017. Characteristics of carbonaceous particles from residential coal combustion and agricultural biomass burning in China. Atmos. Pollut. Res. 8 (3), 521–527.

Travis, K.R., Crawford, J.H., Soja, A.J., et al., 2023. Emission factors for crop residue and prescribed fires in the Eastern US during FIREX-AQ. J. Geophys. Res. Atmos. 128, e2023JD039309.

Van Den Heuvel, R., Staelens, J., Koppen, G., Schoeters, G., 2018. Toxicity of urban PM_{10} and relation with tracers of biomass burning. Int. J. Environ. Res. Publ. Health 15, 320.

Van der Werf, G.R., Randerson, J.T., Giglio, L., van Leeuwen, T.T., Chen, Y., Rogers, B. M., Mu, M., van Marle, M.J.E., Morton, D.C., Collatz, G.J., Yokelson, R.J., Kasibhatla, P.S., 2017. Global fire emissions estimates during 1997–2016. Earth Syst. Sci. Data 9, 697–720.

Van Drooge, B.L., Gromalt, J.O., 2015. Particle size-resolved source apportionment of primary and secondary organic tracer compounds at urban and rural locations in Spain. Atmos. Chem. Phys. 15, 7735–7752.

Vasilakopoulou, C.N., Matrali, A., Skyllakou, K., Georgopoulou, M., Aktypis, A., Florou, K., Kaltsonoudis, C., Siouti, E., Kostenido, E., Błaziak, A., Nenes, A., Papagiannis, S., Eleftheriadis, K., Patoulias, D., Kioutsioukis, I., Pandis, S.N., 2023. Rapid transformation of wildfire emissions to harmful background aerosol. Clim. Atmos. Sci. 6, 218.

Verma, V., Ning, Z., Cho, A.K., Schauer, J.J., Shafer, M.M., Sioutas, C., 2009. Redox activity of urban quasi-ultrafine particles from primary and secondary sources. Atmos. Environ. 43, 6360–6368.

Viana, M., Alastuey, A., Querol, X., Guerreiro, C., Vogt, M., Colette, A., Collet, S., Albinet, A., Fraboulet, I., Lacome, J.M., Tognet, F., de Leeuw, F., 2016. Contribution to residential combustion to ambient air pollution and greenhouse gas emissions. ETC/ACM Technical Paper 2015/1. European Topic Centre on Air Pollution and Climate Change Mitigation,. Netherlands.

Vicente, A., Alves, C., Calvo, A.I., Fernandes, A.P., Nunes, T., Monteiro, C., Marta, S., Pio, C., 2013. Emission factors and detailed chemical composition of smoke particles from the 2010 wildfire season. Atmos. Environ. 71, 295–303.

Vicente, A., Alves, C., Monteiro, C., Nunes, T., Mirante, F., Evtyugina, M., Cerqueira, M., Pio, C., 2011. Measurement of trace gases and organic compounds in the smoke plume from a wildfire in Penedono (central Portugal). Atmos. Environ. 45, 5172–5182.

Vicente, E.D., Alves, C.A., 2018. An overview of particulate emissions from residential biomass combustion. Atmos. Res. 199, 159–185.

Vicente, E.D., Figueiredo, D., Alves, C., 2024. Toxicity of particulate emissions from residential biomass combustion: an overview of *in vitro* studies using cell models. Sci. Total Environ. 927, 171999.

Vicente, E.D., Figueiredo, D., Gonçalves, C., Lopes, I., Oliveira, H., Kováts, N., Pinheiro, T., Alves, C.A., 2021. *In vitro* toxicity of indoor and outdoor PM_{10} from residential wood combustion. Sci. Total Environ. 782, 146820.

Vicente, E.D., Figueiredo, D., Gonçalves, C., Lopes, I., Oliveira, H., Kováts, N., Pinheiro, T., Alves, C.A., 2022. *In vitro* toxicity of particulate matter emissions from residential pellet combustion. J. Environ. Sci. 115, 215–226.

Wang, Y., Plewa, M.J., Mukherjee, U.K., Verma, V., 2018. Assessing the cytotoxicity of ambient particulate matter (PM) using Chinese hamster ovary (CHO) cells and its relationship with the PM chemical composition and oxidative potential. Atmos. Environ. 179, 132–141.

Wang, J., Niu, X., Sun, J., Zhang, Y., Zhang, T., Shen, Z., Zhang, Q., Xu, H., Li, X., Zhang, R., 2020. Source profiles of $PM_{2.5}$ emitted from four typical open burning sources and its cytotoxicity to vascular smooth muscle cells. Sci. Total Environ. 715, 136949.

Weber, S., Salameh, D., Albinet, A., Alleman, L.Y., Waked, A., Besombes, J.-L., Jacob, V., Guillaud, G., Meshbah, B., Rocq, B., Hulin, A., Dominik-Sègue, M., Chrétien, E., Jaffrezo, J.-L., Favez, O., 2019. Comparison of PM_{10} sources profiles at 15 French sites using a harmonized constrained positive matrix factorization approach. Atmosphere 10, 310.

WHO, 2021. Human Health Effects of Polycyclic Aromatic Hydrocarbons as Ambient Air Pollutants: Report of the Working Group on Polycyclic Aromatic Hydrocarbons of the Joint Task Force on the Health Aspects of Air Pollution. World Health Organization Regional Office for Europe, Copenhagen.

Wong, J.P.S., Tsagkaraki, M., Tsiodra, I., Mihalopoulos, N., Violaki, K., Kanakidou, M., Sciare, J., Nenes, A., Weber, R.J., 2019. Effects of atmospheric processing on the oxidative potential of biomass burning organic aerosols. Environ. Sci. Technol. 53, 6747–6756.

Wu, D., Zheng, H., Li, Q., Jin, L., Lyu, R., Ding, X., Huo, Y., Zhao, B., Jiang, J., Chen, J., Li, X., Wang, S., 2022a. Toxic potency-adjusted control of air pollution for solid fuel combustion. Nat. Energy 7, 194–202.

Wu, J., Kong, S., Yan, Y., Cheng, Y., Yan, Q., Liu, D., Wang, S., Zhang, X., Qi, S., 2022b. The toxicity emissions and spatialized health risks of heavy metals in $PM_{2.5}$ from biomass fuels burning. Atmos. Environ. 284, 119178.

Yan, C., Zheng, M., Sullivan, A.P., Bosch, C., Desyaterik, Y., Andersson, A., Li, X., Guo, X., Zhou, T., Gustafsson, Ö., 2015. Chemical characteristics and light-absorbing property of water-soluble organic carbon in Beijing: biomass burning contributions. Atmos. Environ. 121, 4–12.

Yao, W., Zhao, Y., Chen, R., Wang, M., Song, W., Yu, D., 2023. Emissions of toxic substances from biomass burning: a review of methods and technical influencing factors. Processes 11 853.

Yu, S., 2000. Role of organic acids (formic, acetic, pyruvic and oxalic) in the formation of cloud condensation nuclei (CCN): a review. Atmos. Res. 53, 185–217.

Yu, Q., Chen, J., Qin, W., Ahmad, M., Zhang, Y., Sun, Y., Xin, K., Ai, J., 2022. Oxidative potential associated with water-soluble components of $PM_{2.5}$ in Beijing: the important role of anthropogenic organic aerosols. J. Hazard Mater. 433, 128839.

Zhang, H., Hu, J., Qi, Y., Li, C., Chen, J., Wang, X., He, J., Wang, S., Hao, J., Zhang, L., Zhang, L., Zhang, Y., Li, R., Wang, S., Chai, F., 2017. Emission characterization, environmental impact, and control measure of $PM_{2.5}$ emitted from agricultural crop residue burning in China. J. Clean. Prod. 149, 629–635.

Zhang, X., Shi, J., Wang, R., Ma, J., Li, X., Cai, W., Li, T., Zou, W., 2024. Acute exposure to tris(2,4-di-tert-butylphenyl)phosphate elicits cardiotoxicity in zebrafish (*Danio rerio*) larvae via inducing ferroptosis. J. Hazard Mater. 471, 134389.

Zhang, Y., Shao, M., Lin, Y., Luan, S., Mao, N., Chen, W., Wang, M., 2013. Emission inventory of carbonaceous pollutants from biomass burning in the Pearl River Delta Region, China. Atmos. Environ. 76, 189–199.

Zhu, C., Kawamura, K., Kunwar, B., 2015. Effect of biomass burning over the western North Pacific Rim: wintertime maxima of anhydrosugars in ambient aerosols from Okinawa. Atmos. Chem. Phys. 15, 1959–1973.

Zhu, X., Yun, X., Meng, W., Xu, H., Du, W., Shen, G., Cheng, H., Ma, J., Tao, S., 2019. Stacked use and transition trends of rural household energy in mainland China. Environ. Sci. Technol. 53, 521–529.